Figure S1. CTCF binding to the WT *IgH* alleles, related to Figure 1.

Figure S2. Epigenetic features of WT and IGCR1-mutated *IgH* alleles-1, related to Figure 1.

Figure S3. Epigenetic features of WT and IGCR1-mutated *IgH* alleles-2, related to Figure 1.

Figure S4. CTCF- and YY1-dependence of Eμ-V_H81X loop, related to Figure 2.

Figure S5. D_H gene segment utilization on WT and IGCR1-deleted or mutated alleles, related to Figure 3.

Figure S6. V_H recombination efficiency of WT and IGCR1-mutated *IgH* alleles, related to Figure 4.

Figure S7. RAG1/2 binding to IGCR1-deleted *IgH* alleles, related to Figure 5.

Figure S8. Long-distance interactions on IGCR1-mutated *IgH* alleles-1, related to Figure 6.

Figure S9. Long-distance interactions on IGCR1-mutated *IgH* alleles-2, related to Figure 6.

Figure S10. Features of pro-B cells with deletion of proximal V_Hs on WT or IGCR1-mutated *IgH* alleles, related to Figure 6.

Table S1. Average spatial distance and chromatin compaction in the *IgH* locus from different cell lines, related to Figure 1, 2 and 6.

Table S2: V_H7183 usage in IGCR1$^{-/-}$ and WT pro-B cells, related to Figure 3.

Table S3. Primer list, related to Figures 1-6, S1-10.

Table S4. Barcode sequence for different cell lines, related to Figure 6.

Table S5. V_H utilization in different cell lines, related to Figure 6.

Figure S1

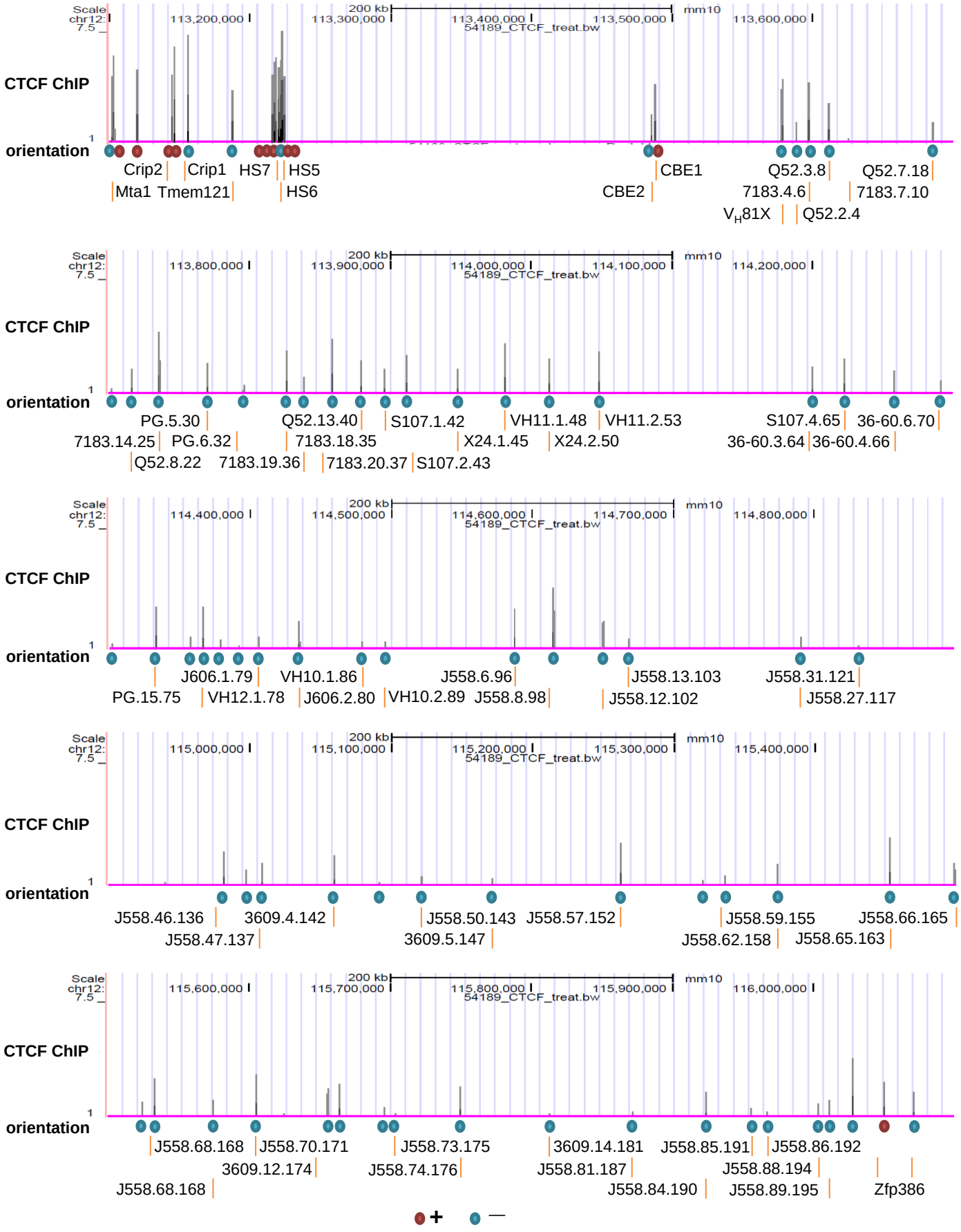
Scale
chr12:
7.5
200 kb
mm10
54189_CTCF_treat.bw
CTCF ChIP
orientation
1
113,200,000
113,300,000
113,400,000
113,500,000
113,600,000
Crip2
Crip1
HS7
HS5
Mta1
Tmem121
HS6
CBE1
CBE2
Q52.3.8
Q52.7.18
7183.4.6
7183.7.10
VH81X
Q52.2.4
113,800,000
113,900,000
114,000,000
114,100,000
114,200,000
PG.5.30
Q52.13.40
S107.1.42
VH11.1.48
VH11.2.53
S107.4.65
36-60.6.70
7183.14.25
PG.6.32
7183.18.35
X24.1.45
X24.2.50
36-60.3.64
36-60.4.66
Q52.8.22
7183.19.36
7183.20.37
S107.2.43
114,400,000
114,500,000
114,600,000
114,700,000
114,800,000
J606.1.79
VH10.1.86
J558.6.96
J558.13.103
J558.31.121
PG.15.75
VH12.1.78
J606.2.80
VH10.2.89
J558.8.98
J558.12.102
J558.27.117
115,000,000
115,100,000
115,200,000
115,300,000
115,400,000
J558.46.136
3609.4.142
J558.50.143
J558.57.152
J558.59.155
J558.66.165
J558.47.137
3609.5.147
J558.62.158
J558.65.163
115,600,000
115,700,000
115,800,000
115,900,000
116,000,000
J558.68.168
J558.70.171
J558.73.175
3609.14.181
J558.85.191
J558.86.192
3609.12.174
J558.74.176
J558.81.187
J558.88.194
J558.68.168
J558.84.190
J558.89.195
Zfp386
+
—

Figure S1. **CTCF binding to the WT *IgH* alleles, related to Figure 1.**

Orientations of CTCF binding sites in *IgH* locus on WT alleles. CTCF ChIP-Seq was extracted from (Lin et al., 2012) (GEO: GSM987805). CTCF binding to the *IgH* locus in pro-B cells is shown by vertical lines. Orientation of CTCF binding sites is noted by blue and red ovals. 11 sites are oriented with the C-rich core on the top strand (+) (red oval) and 75 are oriented with the G-rich core on the bottom strand (-) (blue oval). V_H gene segments are indicated by vertical pink lines.

Figure S2

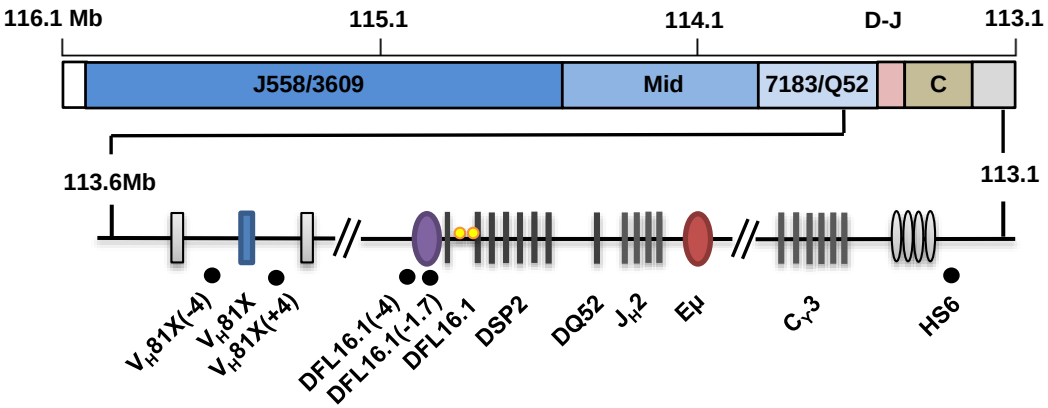
116.1 Mb
115.1
114.1
D-J
113.1
J558/3609
Mid
7183/Q52
C
113.6Mb
113.1
VH81X(-4)
VH81X
VH81X(+4)
DFL16.1(-4)
DFL16.1(-1.7)
DFL16.1
DSP2
DQ52
JH2
Eμ
Cγ3
HS6

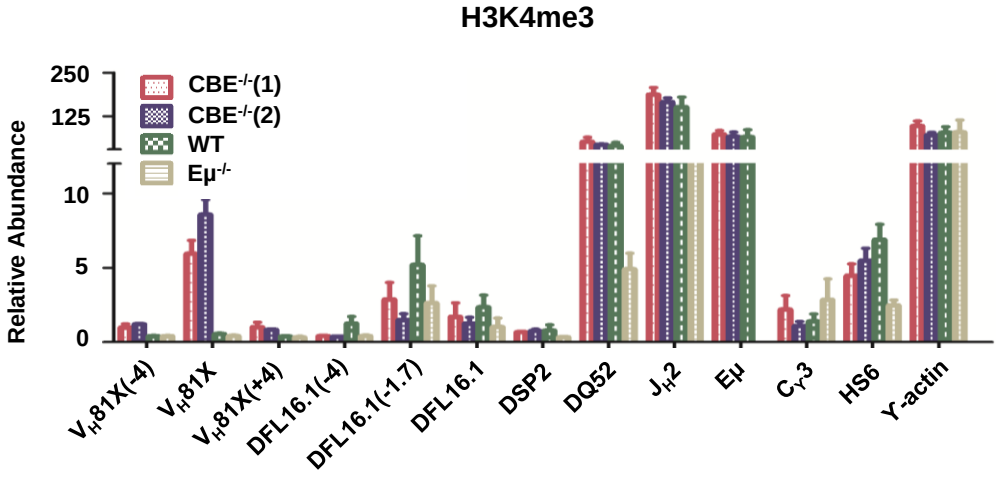
H3K4me3
Relative Abundance
250
125
10
5
0
CBE-/-(1)
CBE-/-(2)
WT
Eμ-/-
VH81X(-4)
VH81X
VH81X(+4)
DFL16.1(-4)
DFL16.1(-1.7)
DFL16.1
DSP2
DQ52
JH2
Eμ
Cγ3
HS6
γ-actin

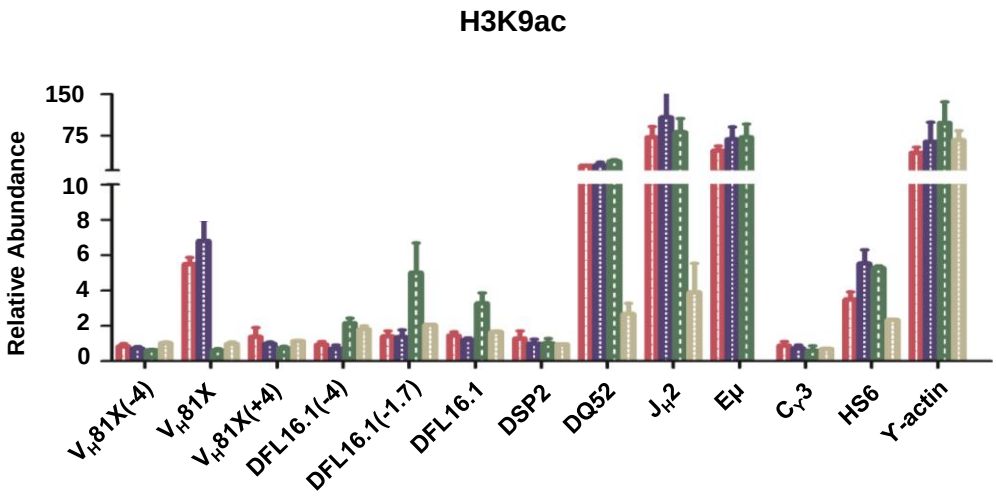
H3K9ac
Relative Abundance
150
75
10
8
6
4
2
0
VH81X(-4)
VH81X
VH81X(+4)
DFL16.1(-4)
DFL16.1(-1.7)
DFL16.1
DSP2
DQ52
JH2
Eμ
Cγ3
HS6
γ-actin

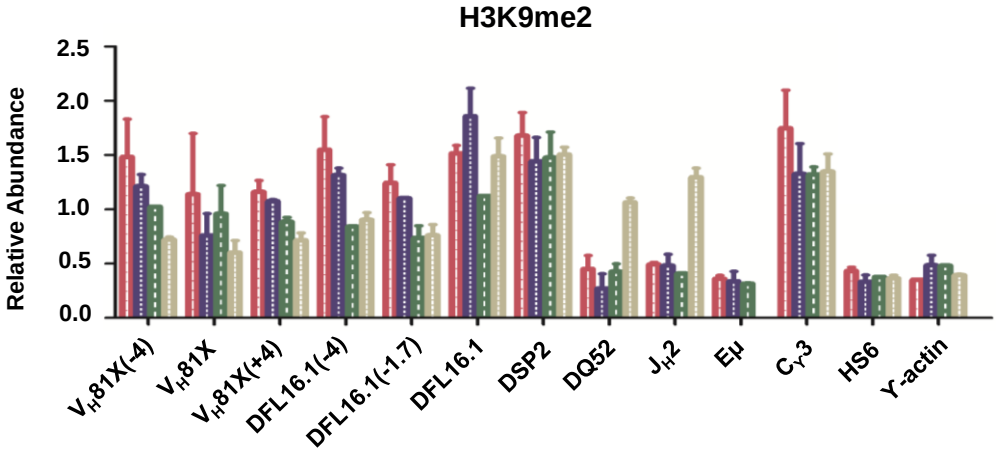
H3K9me2
Relative Abundance
2.5
2.0
1.5
1.0
0.5
0.0
VH81X(-4)
VH81X
VH81X(+4)
DFL16.1(-4)
DFL16.1(-1.7)
DFL16.1
DSP2
DQ52
JH2
Eμ
Cγ3
HS6
γ-actin

Figure S2. **Epigenetic features of WT and IGCR1-mutated *IgH* alleles-1, related to Figure 1.**

IGCR1-mutated *IgH* alleles. Four RAG2-deficient pro-B cell lines containing wild-type *IgH* alleles (WT), IGCR1-mutated *IgH* alleles ($CBE^{-/-}$(1) and (2)), and Eμ-deficient *IgH* alleles ($E\mu^{-/-}$), were used in chromatin immunoprecipitation (ChIP) assays using anti-H3K4me3, anti-H3K9ac and anti-H3K9me2 antibodies as previously described (Chakraborty et al., 2007; Chakraborty et al., 2009; Subrahmanyam et al., 2012). Positions of amplicons are indicated in the schematic on the top line. V_H81X(-4) and V_H81X(+4) are located approximately 4 kb 5' or 3' of V_H81X, respectively. HS6 is located 5 kb from HS4. Relative abundance (Y axis) of each amplicon in the immunoprecipitate was calculated relative to an equal amount (200 pg) of input DNA. Data are shown as mean ± SEM of two or three independent ChIP experiments in each cell line. ChIP amplicons were assayed in duplicates.

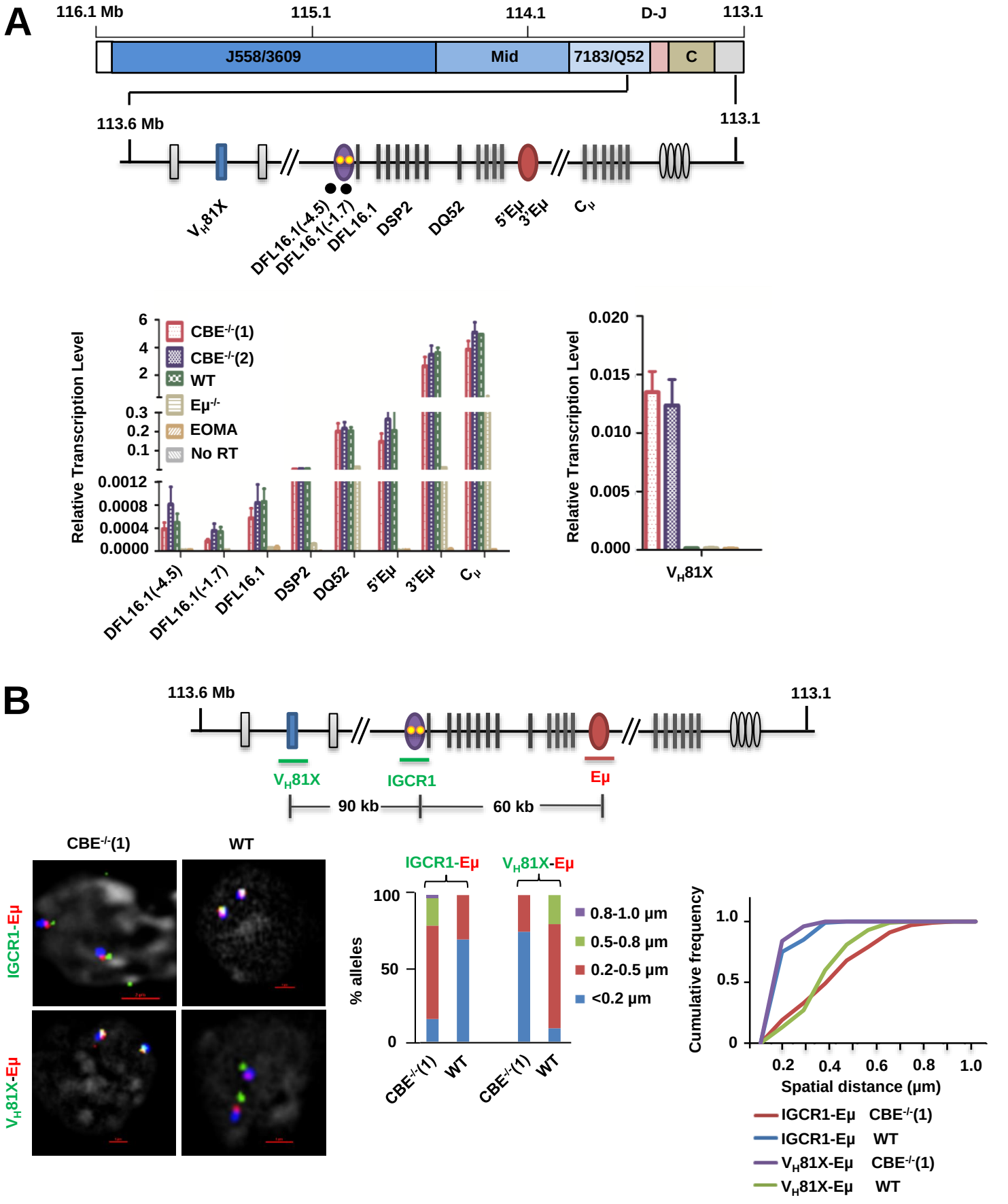
A
116.1 Mb
115.1
114.1
D-J
113.1
J558/3609
Mid
7183/Q52
C
113.6 Mb
113.1
VH81X
DFL16.1(-4.5)
DFL16.1(-1.7)
DFL16.1
DSP2
DQ52
5'Eμ
3'Eμ
Cμ
Relative Transcription Level
CBE-/-(1)
CBE-/-(2)
WT
Eμ-/-
EOMA
No RT
B
113.6 Mb
113.1
VH81X
IGCR1
Eμ
90 kb
60 kb
CBE-/-(1)
WT
IGCR1-Eμ
VH81X-Eμ
% alleles
0.8-1.0 μm
0.5-0.8 μm
0.2-0.5 μm
<0.2 μm
Cumulative frequency
Spatial distance (μm)
IGCR1-Eμ CBE-/-(1)
IGCR1-Eμ WT
VH81X-Eμ CBE-/-(1)
VH81X-Eμ WT

Figure S3. **Epigenetic features of WT and IGCR1-mutated *IgH* alleles-2, related to Figure 1.**

A. Transcription of WT and IGCR1-mutated *IgH* alleles. Total RNA from 4 cell lines described in Figure S2, together with EOMA (a non-B cell line of endothelial origin from 129 strain), was reverse transcribed with random hexamer primers and assayed by qPCR. No RT served as a control. Positions of amplicons are indicated in the schematic on the top line. DFL16.1 (-4.5) and DFL16.1 (-1.7) are located 4.5 kb and 1.7 kb 5'of DFL16.1, respectively. Relative transcript level (Y axis) was calculated according to the formula $2^{(Ct_{gene}-Ct_{\gamma\text{-}actin})}$, with *γ-actin* mRNA serving to normalize between samples. Data are shown as mean ± SEM of two independent RNA preparations from each cell line.

B. FISH analyses of WT and IGCR1-mutated alleles. Biological replicate of the experiment described in Figure 1C. Spatial distance measurements and quantitation was done as described in Figure 1C legend.

Figure S4

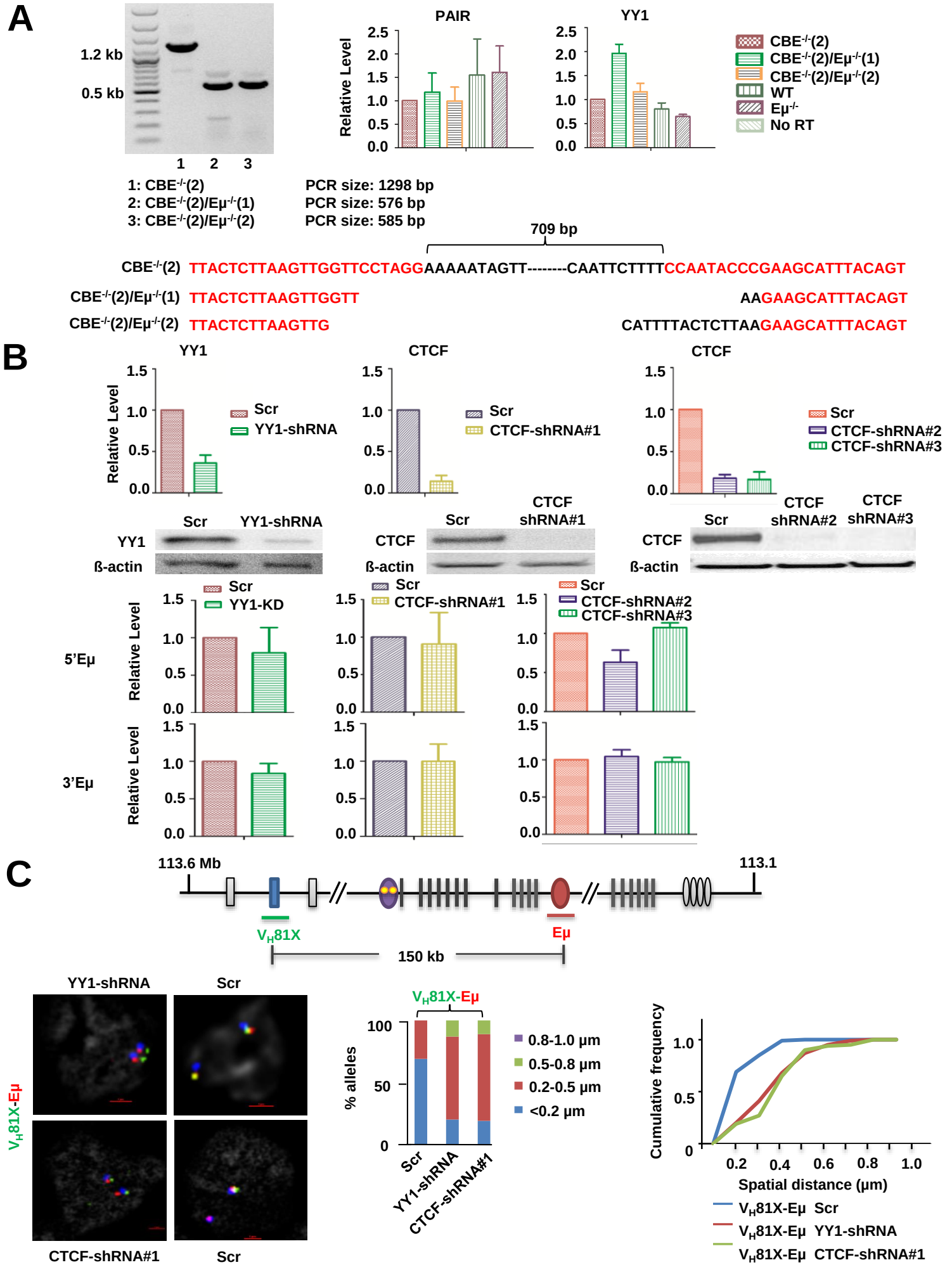
A
1.2 kb
0.5 kb
1 2 3
1: CBE-/-(2)
2: CBE-/-(2)/Eμ-/-(1)
3: CBE-/-(2)/Eμ-/-(2)
PAIR
YY1
Relative Level
CBE-/-(2)
CBE-/-(2)/Eμ-/-(1)
CBE-/-(2)/Eμ-/-(2)
WT
Eμ-/-
No RT
PCR size: 1298 bp
PCR size: 576 bp
PCR size: 585 bp
709 bp
CBE-/-(2) TTACTCTTAAGTTGGTTCCTAGGAAAAATAGTT--------CAATTCTTTTCCAATACCCGAAGCATTTACAGT
CBE-/-(2)/Eμ-/-(1) TTACTCTTAAGTTGGTT AAGAAGCATTTACAGT
CBE-/-(2)/Eμ-/-(2) TTACTCTTAAGTTG CATTTTACTCTTAAGAAGCATTTACAGT
B
YY1
CTCF
CTCF
Scr
YY1-shRNA
CTCF-shRNA#1
CTCF-shRNA#2
CTCF-shRNA#3
YY1
CTCF
ß-actin
CTCF shRNA#1
CTCF shRNA#2
CTCF shRNA#3
YY1-KD
5'Eμ
3'Eμ
C
113.6 Mb
113.1
VH81X
Eμ
150 kb
YY1-shRNA
Scr
CTCF-shRNA#1
VH81X-Eμ
% alleles
0.8-1.0 μm
0.5-0.8 μm
0.2-0.5 μm
<0.2 μm
Cumulative frequency
Spatial distance (μm)
VH81X-Eμ Scr
VH81X-Eμ YY1-shRNA
VH81X-Eμ CTCF-shRNA#1

Figure S4. CTCF- and YY1-dependence of Eμ-V_H81X loop, related to Figure 2.

A. Generation and characterization of IGCR1-mutated and Eμ-deleted *IgH* alleles. gRNAs (Table S3) were used to delete Eμ in the $CBE^{-/-}$(2) cell line that contains IGCR1-mutated *IgH* alleles. Two subclones were further characterized for functional studies. Homozygous Eμ deletion was ascertained by PCR followed by sequencing of the deletion junction (lower panel). Total RNA isolated from $CBE^{-/-}$(2), $CBE^{-/-}$(2)/$Eμ^{-/-}$(1), $CBE^{-/-}$(2)/$Eμ^{-/-}$(2), WT or $Eμ^{-/-}$ cells was assayed by quantitative RT-PCR using amplicons from *IgH*-associated PAIR elements (Ebert et al., 2011) and *Yy1* gene. No RT refers to cDNA synthesis without adding reverse transcriptase. Data are shown as mean ± SEM of two independent RNA preparations from each cell line.

B. Characterization of YY1- and CTCF-knockdown (KD) cells. $CBE^{-/-}$(2) cells were infected with lentiviruses carrying shRNAs targeted to *Yy1* or *Ctcf* mRNA, or a scrambled (Scr) shRNA to serve as a negative control. After 5 days selection in puromycin, Total RNA isolated from KD or control cells was assayed by qPCR by quantitation of *Yy1*, *Ctcf*, and Eμ transcripts (5′Eμ and 3′Eμ expression). Transcript levels were normalized to *γ-actin* mRNA and are represented relative to levels in control cells (Y axis). Data are shown as mean ± SEM of two or three independent knock-down experiments followed by RNA analysis. Whole cell extracts from KD or control cells were assayed by immunoblotting using antibodies against YY1, CTCF or ß-actin. ß-actin served as a loading control. Data are shown as mean ± SEM of two independent knockdown experiments.

C. FISH analyses of Eμ-V_H81X loop in KD and control (Scr) cells. Biological replicate experiments were done as described in Figure 2B.

Figure S5

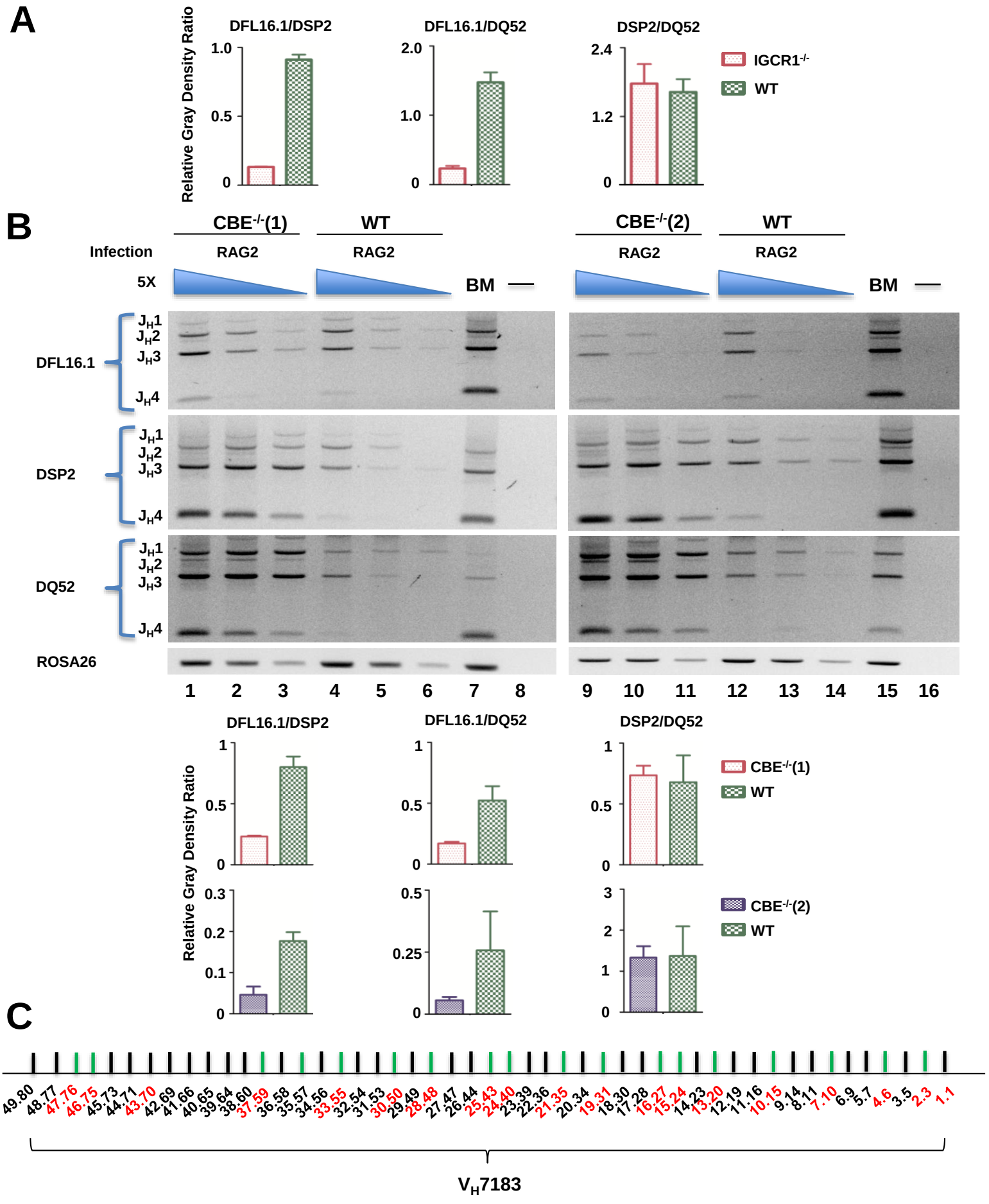
A
DFL16.1/DSP2
DFL16.1/DQ52
DSP2/DQ52
Relative Gray Density Ratio
IGCR1-/-
WT
B
CBE-/-(1)
WT
CBE-/-(2)
WT
Infection
RAG2
5X
BM
DFL16.1
DSP2
DQ52
ROSA26
JH1
JH2
JH3
JH4
1 2 3 4 5 6 7 8 9 10 11 12 13 14 15 16
CBE-/-(1)
CBE-/-(2)
C
49.80 48.77 47.76 46.75 45.73 44.71 43.70 42.69 41.66 40.65 39.64 38.60 37.59 36.58 35.57 34.56 33.55 32.54 31.53 30.50 29.49 28.48 27.47 26.44 25.43 24.40 23.39 22.36 21.35 20.34 19.31 18.30 17.28 16.27 15.24 14.23 13.20 12.19 11.16 10.15 9.14 8.11 7.10 6.9 5.7 4.6 3.5 2.3 1.1
VH7183

Figure S5. D_H gene segment utilization on WT and IGCR1-deleted or mutated alleles, related to Figure 3.

A. Quantitation of D_H rearrangements in bone marrow pro-B cells carrying WT and IGCR1-deleted *IgH* alleles. D_H-J_H4 rearrangements shown in Figure 3A were scanned and analyzed with gray density analysis software (GeneTools from Syngene). For each D_H gene segment, the total intensity of bands corresponding to rearrangements to J_H1-4 was obtained from lanes 2 and 5 (Figure 3A). Bar graphs show the ratio of DFL16.1 to DSP2, as well as DQ52 rearrangements within each genotype (left and middle); the ratios of DSP2 to DQ52 rearrangements are shown on the right. Data are shown as mean ± SEM of two rearrangement assays from independent pro-B cell sorts.

B. RAG2-deficient pro-B cell lines, $CBE^{-/-}$(1) and (2), and WT, were infected with *Rag2*-expressing lentivirus or control lentivirus. After 4 or 5 days of selection with puromycin, genomic DNA was prepared to assay rearrangements. D_H-J_H4 rearrangements were amplified and analyzed by agarose gel electrophoresis. 5-fold decreasing amounts of genomic DNA starting at 200ng (lanes 1, 4, 9 and 12) are shown for each genotype. The non-rearranging ROSA26 locus served as a loading control. Upper panel, rearrangements of each D_H gene segment to the four J_H gene segments are shown. Lower panel, gray density (lane 2, 5, 10 and 13) was calculated as described for part A, and ratios of DFL16.1/DSP2, DFL16.1/DQ52 and DSP2/DQ52 are shown. Data are shown as mean ± SEM of two independent infections of each cell line followed by rearrangement assays.

C. Schematic map of V_H7183 gene family. 19 (red) out of total 49 V_H genes are recognized by the V_H7183 primer used in the rearrangement assays. Sequence of V_H7183 primer is listed in Table S3. Green and black lines stand for functional and non-functional genes, respectively (Retter et al., 2007).

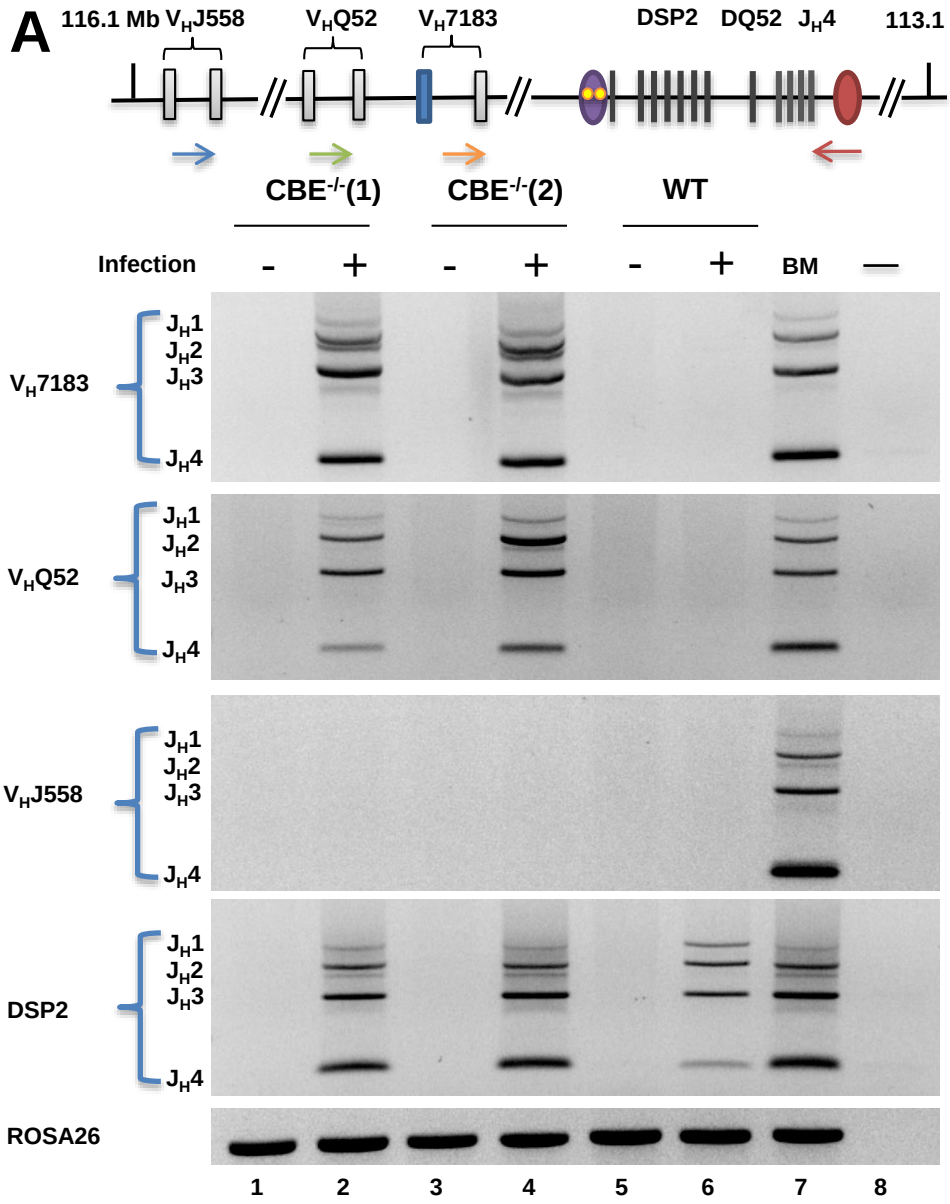
A
116.1 Mb VHJ558
VHQ52
VH7183
DSP2
DQ52
JH4
113.1
CBE-/-(1)
CBE-/-(2)
WT
Infection
- + - + - + BM —
VH7183
VHQ52
VHJ558
DSP2
JH1
JH2
JH3
JH4
ROSA26
1 2 3 4 5 6 7 8

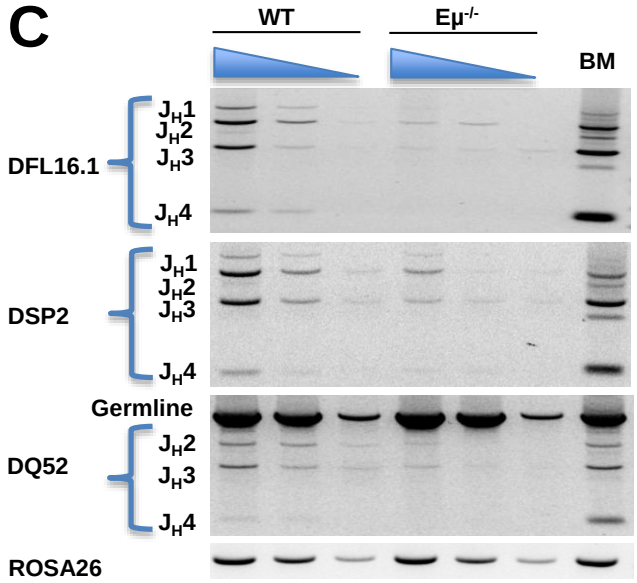
C
WT
Eμ-/-
BM
DFL16.1
DSP2
Germline
DQ52
ROSA26
JH1
JH2
JH3
JH4

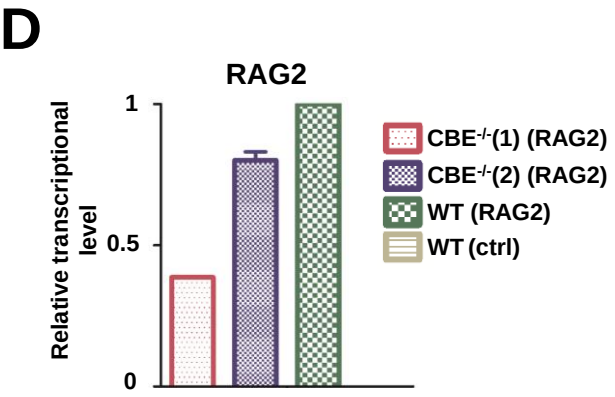
D
RAG2
Relative transcriptional level
1
0.5
0
CBE-/-(1) (RAG2)
CBE-/-(2) (RAG2)
WT (RAG2)
WT (ctrl)

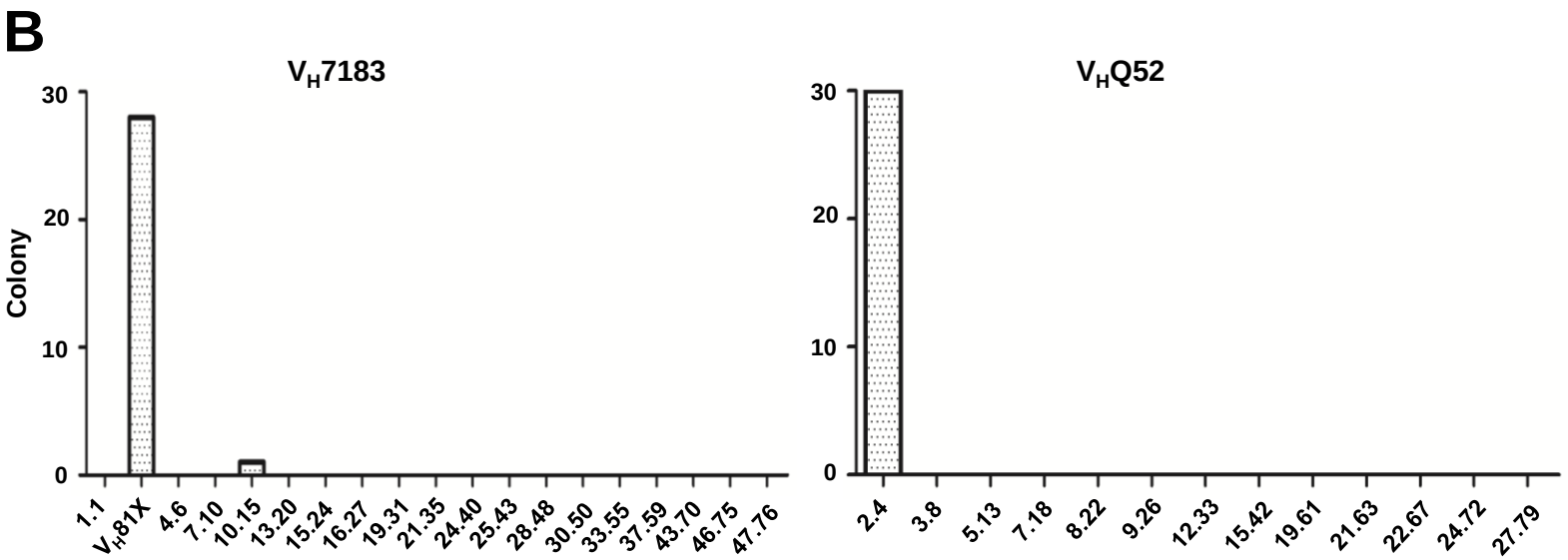
B
VH7183
VHQ52
Colony
30
20
10
0
1.1
VH81X
4.6
7.10
10.15
13.20
15.24
16.27
19.31
21.35
24.40
25.43
28.48
30.50
33.55
37.59
43.70
46.75
47.76
2.4
3.8
5.13
7.18
8.22
9.26
12.33
15.42
19.61
21.63
22.67
24.72
27.79

Figure S6. V_H recombination efficiency of WT and IGCR1-mutated *IgH* alleles, related to Figure 4.

A. RAG2-deficient pro-B cell lines carrying IGCR1-mutated alleles ($CBE^{-/-}$(1) and (2)) or WT *IgH* alleles (WT) were infected with *Rag2*-expressing lentivirus or control lentivirus. After 14 days of selection with puromycin, genomic DNA was prepared for rearrangement. Genomic DNA purified from these cells was used in amplification reactions with a 5' primer that scores for V_HJ558 (blue), V_HQ52 (green), or V_H7183 (orange) together with a 3' primer located beyond J_H4 (red). Amplification products were analyzed by agarose gel electrophoresis. The non-rearranging ROSA26 locus served as a loading control. Lane 7 is positive control using bone marrow genomic DNA; lane 8 contains no genomic DNA. Data shown is representative of two independent infections followed by analyses of recombination.

B. RAG2-deficient pro-B cell line carrying IGCR1-mutated *IgH* alleles ($CBE^{-/-}$(1)) was infected with *Rag2* expressing lentivirus. After 14 days of selection with puromycin, genomic DNA was prepared for rearrangement. Genomic DNA purified from these cells was used in amplification reactions with a 5' primer that scores for 19 V_H7183 gene segments, or 13 V_HQ52 gene segments together with a 3' primer located beyond J_H1. Amplification products were sub-cloned into pGEM®-T, and 29 (V_H7183) or 30 (V_HQ52) clones were sequenced to estimate V_H and D_H usage. Numbers of clones with V_H7183 (left) and V_HQ52 (right) rearrangements are shown in the graph.

C. RAG2-deficient pro-B cell lines carrying WT *IgH* alleles (WT) or Eμ deficient alleles ($E\mu^{-/-}$) were infected with *Rag2* expressing lentivirus or control lentivirus. After 14 days of selection with puromycin, genomic DNA purified from these cells was used in amplification reactions with a 5' primer that scores for DFL16.1, DSP2 or DQ52 together with a 3' primer located beyond J_H4 (red). Amplification products were analyzed by agarose gel electrophoresis. The non-rearranging ROSA26 locus served as a loading control. Data shown is representative of two independent infections followed by analyses of recombination.

D. Total RNA from cell lines described in part A was reverse transcribed with random hexamer primers, and transcriptional levels of *Rag2* were normalized to *γ-actin* mRNA and are represented relative to levels in WT cells (Y axis). WT (ctrl) represents the starting RAG2-deficient pro-B cell line with WT *IgH* alleles after transduction with a control virus. Data are shown as mean ± SEM of two independent experiments.

Figure S7

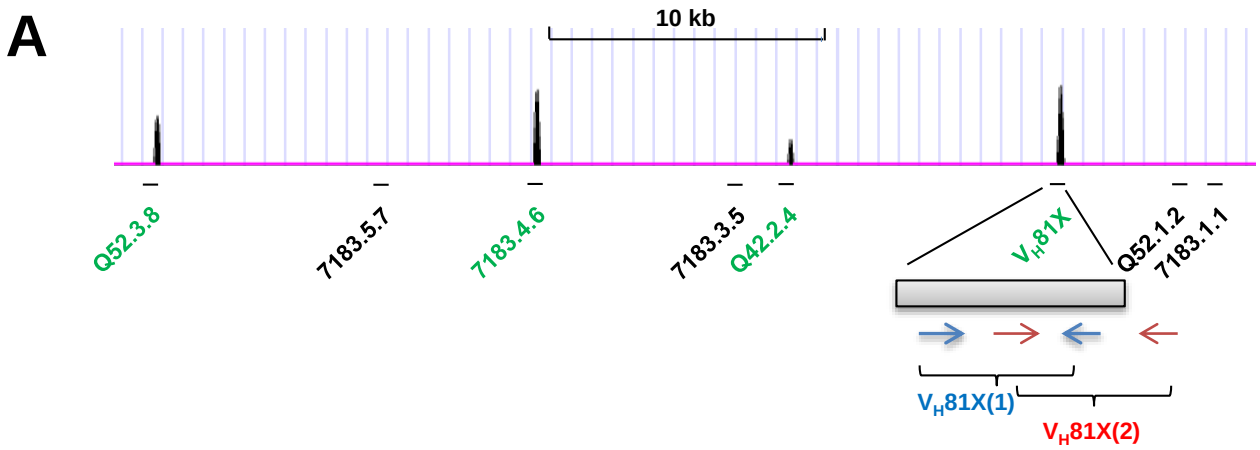
A
10 kb
Q52.3.8
7183.5.7
7183.4.6
7183.3.5
Q42.2.4
VH81X
Q52.1.2
7183.1.1
VH81X(1)
VH81X(2)

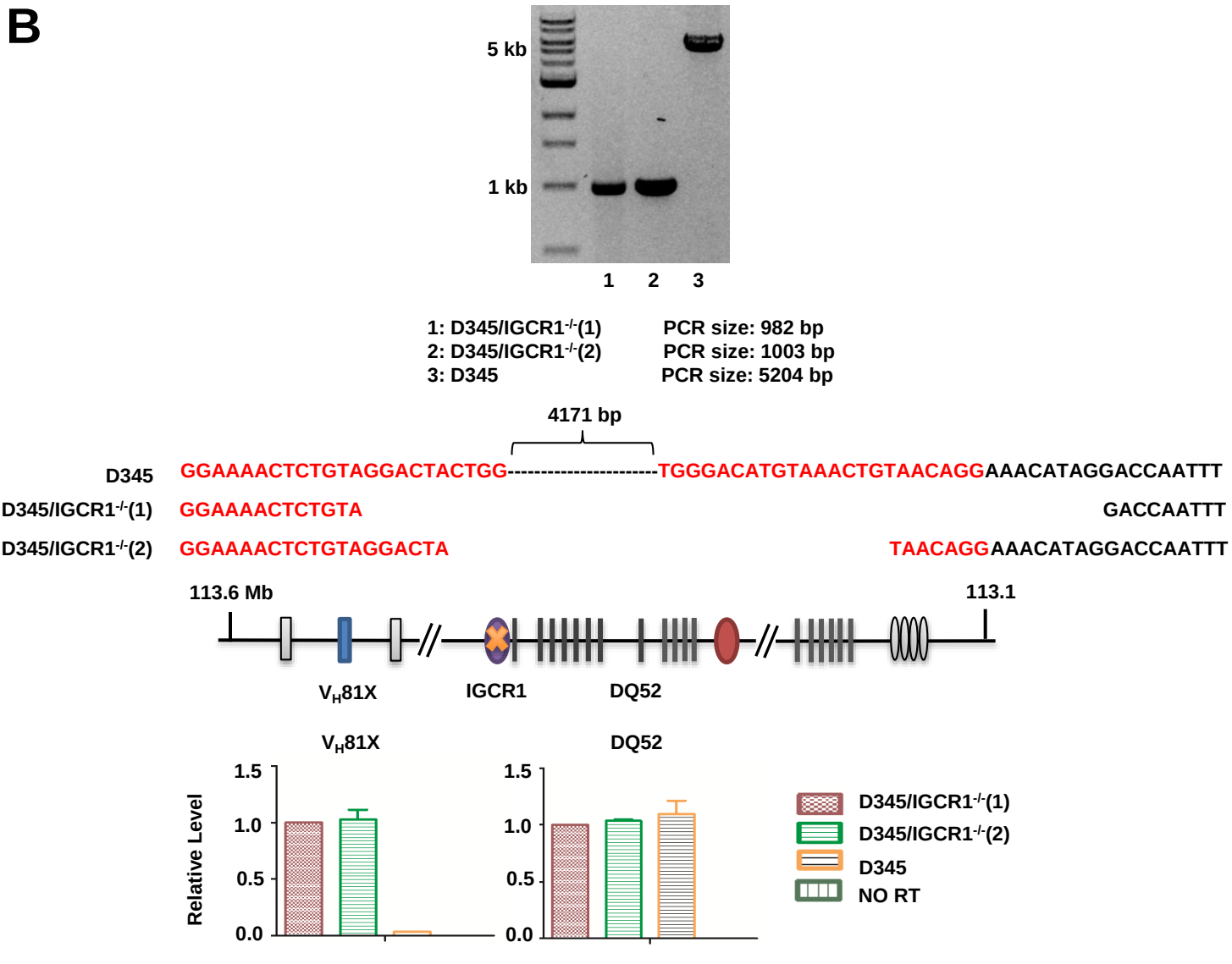
B
5 kb
1 kb
1 2 3
1: D345/IGCR1-/-(1) PCR size: 982 bp
2: D345/IGCR1-/-(2) PCR size: 1003 bp
3: D345 PCR size: 5204 bp
4171 bp
D345 GGAAAACTCTGTAGGACTACTGG----------TGGGACATGTAAACTGTAACAGGAAACATAGGACCAATTT
D345/IGCR1-/-(1) GGAAAACTCTGTA GACCAATTT
D345/IGCR1-/-(2) GGAAAACTCTGTAGGACTA TAACAGGAAACATAGGACCAATTT
113.6 Mb
113.1
VH81X
IGCR1
DQ52
VH81X
DQ52
Relative Level
1.5
1.0
0.5
0.0
D345/IGCR1-/-(1)
D345/IGCR1-/-(2)
D345
NO RT

Figure S7. RAG1/2 binding to IGCR1-deleted *IgH* alleles, related to Figure 5.

A. Location of ChIP amplicons and CTCF binding sites within proximal V_H genes. CTCF ChIP-Seq data was derived from previous published data (Lin et al., 2012). Locations of seven of the 3'-most V_H gene segments are shown below the line. V_HQ52.1.2 and V_H7183.1.1 are pseudogenes; V_H81X is the 3'-most functional V_H gene segment. Expanded view below V_H81X shows positioning of primer pairs for V_H81X(1)and V_H81X(2) amplicons. The 3' primer of V_H81X(2) amplicon ensures detection of only unrearranged V_H81X gene segments.

B. Generation and characterization of IGCR1-deleted derivatives of the pro-B cell line D345 that expresses catalytically inactive RAG1 and endogenous RAG2. gRNAs listed in Table S3 were used to delete IGCR1 using CRISPR/Cas9. PCR was employed to show the deletion of IGCR1. Two subclones, D345/IGCR1$^{-/-}$(1) and D345/IGCR1$^{-/-}$(2), were selected for further analyses. PCR assays using primers flanking IGCR1 confirmed homozygous deletion of approximately 4 kb. PCR products were subcloned and sequenced to obtain precise junctional information. Total RNA isolated from D345/IGCR1$^{-/-}$(1), D345/IGCR1$^{-/-}$(2) cells was assayed by quantitative RT-PCR to examine V_H81X and DQ52 transcripts. cDNA synthesis without the addition of reverse transcription polymerase is indicated as No RT. Transcript levels were normalized to *γ-actin* mRNA and are shown relative to levels in D345/IGCR1$^{-/-}$(1) cells (Y axis). Data are shown as mean ± SEM of two independent experiments.

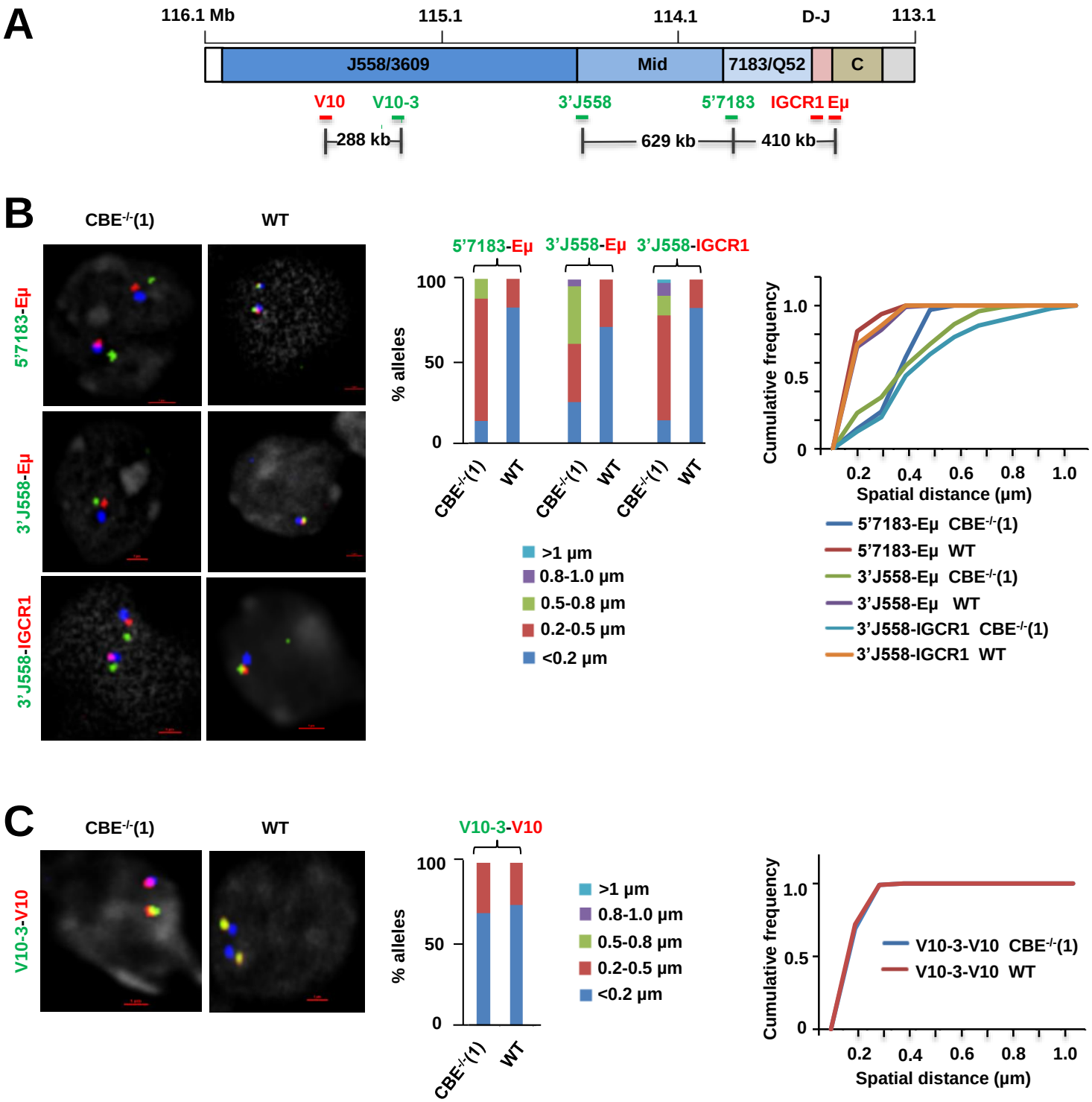
A
116.1 Mb
115.1
114.1
D-J
113.1
J558/3609
Mid
7183/Q52
C
V10
V10-3
3'J558
5'7183
IGCR1
Eμ
288 kb
629 kb
410 kb
B
CBE-/-(1)
WT
5'7183-Eμ
3'J558-Eμ
3'J558-IGCR1
% alleles
100
50
0
>1 μm
0.8-1.0 μm
0.5-0.8 μm
0.2-0.5 μm
<0.2 μm
Cumulative frequency
1.0
0.5
0
0.2
0.4
0.6
0.8
1.0
Spatial distance (μm)
5'7183-Eμ CBE-/-(1)
5'7183-Eμ WT
3'J558-Eμ CBE-/-(1)
3'J558-Eμ WT
3'J558-IGCR1 CBE-/-(1)
3'J558-IGCR1 WT
C
V10-3-V10

Figure S8. Long-distance interactions on IGCR1-mutated *IgH* alleles-1, related to Figure 6.

A and B. Biological replicates of experiments described in Figure 6.

C. Structure of the V_H locus. A CTCF-dependent interaction in the distal V_H locus was measured using probes V10-3 and V10 in RAG2-deficient pro-B cell lines with WT and IGCR1-mutated ($CBE^{-/-}$(1)) *IgH* alleles (top panel). BAC RP23-201H14 is in blue. Representative nuclei are shown with probe combination indicated on the left. Spatial distance measurements from 100 nuclei of each genotype are summarized in the bar graph and cumulative frequency plots as described in Figure 6B. At least two independent FISH experiments were carried out with each probe combination.

Figure S9

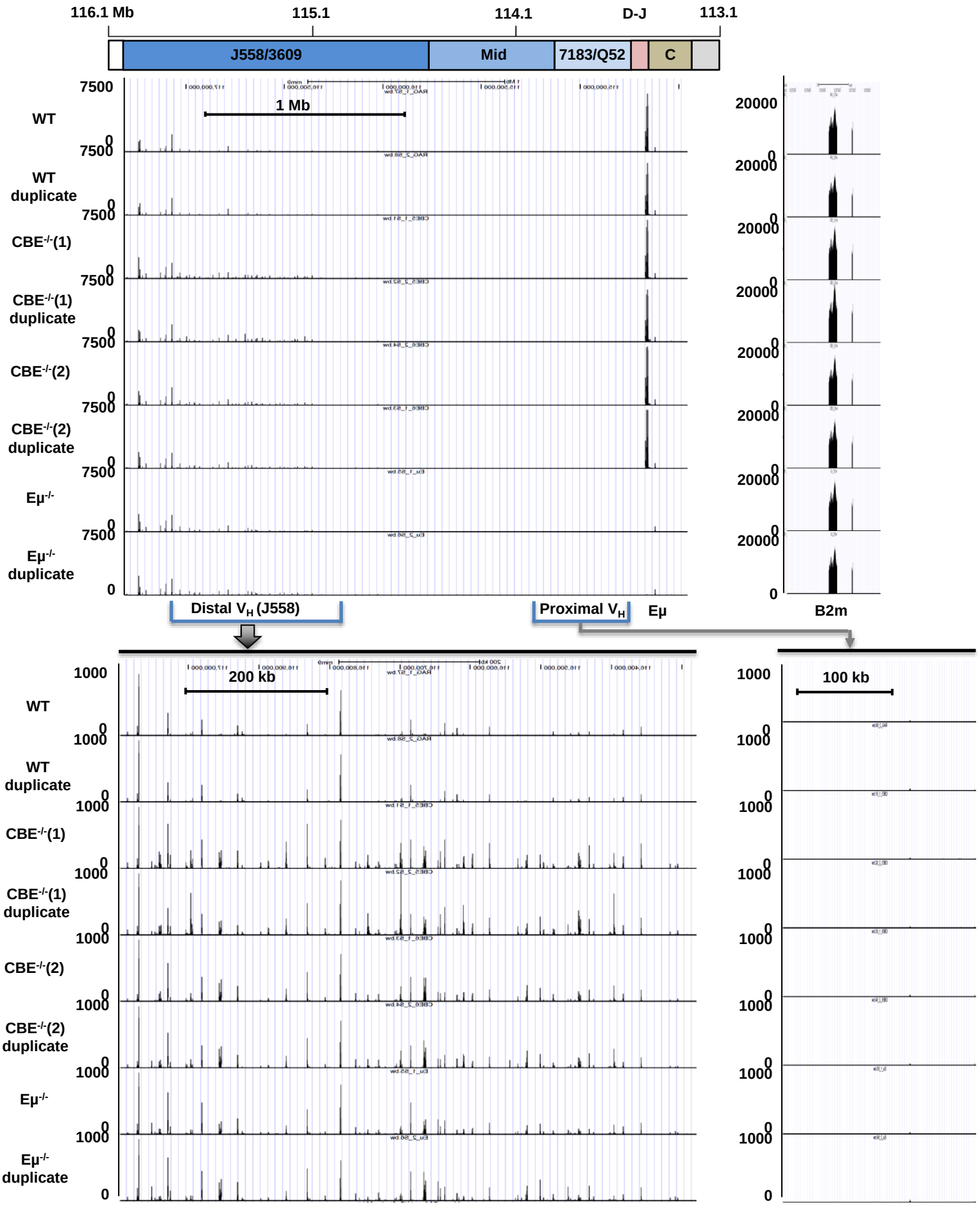
116.1 Mb
115.1
114.1
D-J
113.1
J558/3609
Mid
7183/Q52
C
1 Mb
WT
WT duplicate
CBE-/-(1)
CBE-/-(1) duplicate
CBE-/-(2)
CBE-/-(2) duplicate
Eμ-/-
Eμ-/- duplicate
7500
0
20000
Distal VH (J558)
Proximal VH
Eμ
B2m
200 kb
100 kb
1000

Figure S9. Long-distance interactions on IGCR1-mutated *IgH* alleles-2, related to Figure 6.

RNA-Seq analysis of different cell lines with WT or IGCR1-mutated alleles. $CBE^{-/-}$(1) and $CBE^{-/-}$(2) carry mutations in IGCR1 whereas $E\mu^{-/-}$ lacks the intronic enhancer. The entire *IgH* locus (Ch12: 114,452,000 - 117,310,000) in mm9 is shown in the top half. B2m (Chr2: 121,975,206 - 121,978,345) was used as a control. Parts of the locus comprising distal V_H locus (Ch12: 116,276,841-117,096,033) and proximal V_H locus (chr12: 114,800,000 - 115,000,000) are shown in the bottom part of this figure. Duplicate experiments were carried out and results from each replicate are shown.

Figure S10

A

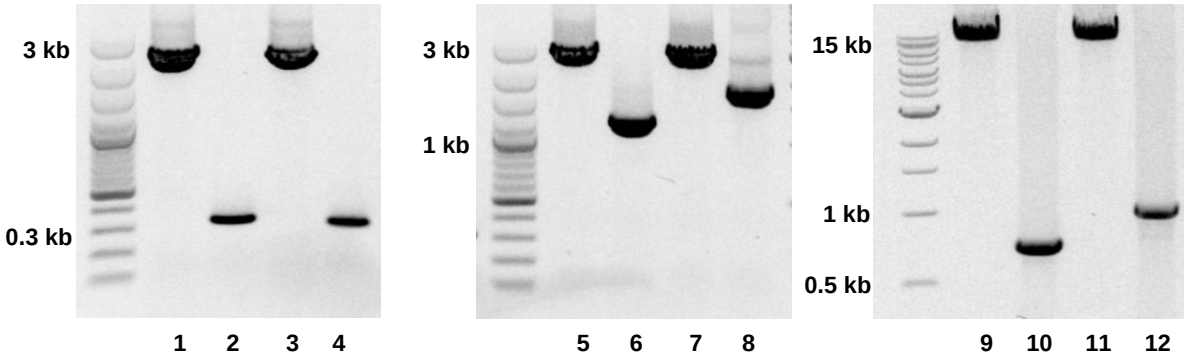

1: CBE$^{-/-}$(1) PCR size: 2491 bp
2: CBE$^{-/-}$(1)/C1$^{-/-}$ PCR size: 338 bp
3: WT PCR size: 2491 bp
4: WT/C1$^{-/-}$ PCR size: 323 bp
5: CBE$^{-/-}$(1) PCR size: 3025 bp
6: CBE$^{-/-}$(1)/C2$^{-/-}$ PCR size: 1237 bp
7: WT PCR size: 3025 bp
8: WT/C2$^{-/-}$ PCR size: 1881 bp
9: CBE$^{-/-}$(1) PCR size: 12790 bp
10: CBE$^{-/-}$(1)/C1$^{-/-}$C2$^{-/-}$ PCR size: 727 bp
11: WT PCR size: 12790 bp
12: WT/C1$^{-/-}$C2$^{-/-}$ PCR size: 1 kb

B

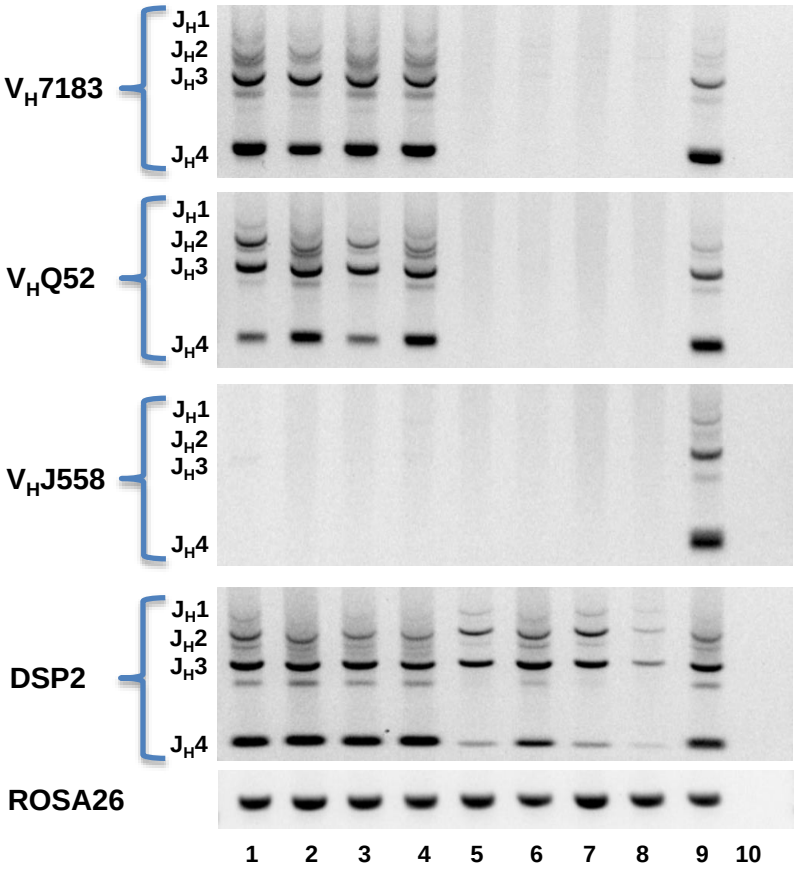

1: CBE$^{-/-}$(1)
2: CBE$^{-/-}$(1)/C1$^{-/-}$
3: CBE$^{-/-}$(1)/C2$^{-/-}$
4: CBE$^{-/-}$(1)/C1$^{-/-}$C2$^{-/-}$
5: WT
6: WT/C1$^{-/-}$
7: WT/C2$^{-/-}$
8: WT/C1$^{-/-}$C2$^{-/-}$
9: BM
10: H2O

Figure S10. Features of pro-B cells with deletion of proximal V_Hs on WT or IGCR1-mutated *IgH* alleles, related to Figure 6.

A. Generation and characterization of different pro-B cell lines. gRNAs listed in Table S3 were used to delete C1 (left), C2 (middle) or C1andC2 (right) on WT or IGCR1 mutated alleles using CRISPR/Cas9. PCR assays using primers flanking C1, C2 or C1C2 confirmed homozygous deletion. PCR products were subcloned into pGEM®-T and sequenced to obtain precise junctional information. PCR size information of different cell lines are listed below of the gel.

B. Pro-B cell lines with different *IgH* genotypes as labeled were infected with *Rag2* expressing lentivirus. After 10 days of selection with puromycin, genomic DNA purified from these cells was used in amplification reactions with a 5' primer that scores for V_HJ558, V_HQ52, V_H7183 or DSP2 together with a 3' primer located beyond J_H4. Amplification products were analyzed by agarose gel electrophoresis. The non-rearranging ROSA26 locus served as a loading control. Lanes 9 is the positive control using bone marrow genomic DNA; lanes 10 contain no genomic DNA. Data shown is representative of two independent infections followed by analyses of recombination.

Table S1. Average spatial distance and chromatin compaction in the *IgH* locus from different cell lines, related to Figure 1, 2 and 6.

Probes	Genomic Distance (Mb)	Number of Alleles	Spatial Distance± SD in µm	Compaction[a]	Genotype	D-statistic (K-S test)	P-value
IGCR1-Eµ	0.06	106	0.319±0.168	64	$CBE^{-/-}$(1)		
IGCR1-Eµ	0.06	105	0.161±0.067	127	WT	0.49847	8.25E-12
V_H81X-Eµ	0.15	100	0.141±0.042	362	$CBE^{-/-}$(1)		
V_H81X-Eµ	0.15	100	0.309±0.206	165	WT	0.53	1.26E-12
V_H81X-Eµ	0.15	100	0.156±0.055	327	Scr		
V_H81X-Eµ	0.15	100	0.350±0.146	146	YY1-shRNA	0.65	< 2.2e-16
V_H81X-Eµ	0.15	100	0.347±0.172	147	CTCF-shRNA#1	0.63	< 2.2e-16
5'7183-Eµ	0.41	100	0.467±0.227	299	$CBE^{-/-}$(1)		
5'7183-Eµ	0.41	100	0.175±0.083	797	WT	0.65	< 2.2e-16
3'J558-Eµ	1.04	100	0.390±0.202	907	$CBE^{-/-}$(1)		
3'J558-Eµ	1.04	100	0.199±0.118	1777	WT	0.51	1.01E-11
3'J558-IGCR1	0.98	100	0.475±0.246	701	$CBE^{-/-}$(1)		
3'J558-IGCR1	0.98	100	0.184±0.092	1811	WT	0.66	< 2.2e-16
V10-3-V10	0.50	100	0.140±0.057	1214	$CBE^{-/-}$(1)		
V10-3-V10	0.50	100	0.137±0.054	1241	WT	0.09	0.8127

[a]Compaction Value: 340 [nm] x genomic length [kb] / spatial distance [nm] x 1 kb

Table S2: V_H7183 usage in IGCR1$^{-/-}$ and WT pro-B cells, related to Figure 3.

	IGCR1$^{-/-}$(1)		IGCR1$^{-/-}$(2)		WT(1)		WT(2)	
V_H7183 family	Colony	Percentage	Colony	Percentage	Colony	Percentage	Colony	Percentage
V_H7183.1.1	2	3.6%	4	7.1%				
V_H7183.2.3	52	94.6%	50	89.3%	19	33.9%	6	10.9%
V_H7183.4.6			1	1.8%	9	16.1%	7	12.7%
V_H7183.7.10					4	7.1%	2	3.6%
V_H7183.10.15							1	1.8%
V_H7183.13.20					4	7.1%	8	14.5%
V_H7183.15.24					3	5.4%	6	10.9%
V_H7183.19.31					3	5.4%	2	3.6%
V_H7183.21.35			1	1.8%			6	10.9%
V_H7183.24.40					3	5.4%	1	1.8%
V_H7183.25.43							2	3.6%
V_H7183.28.48					2	3.6%		
V_H7183.30.50					1	1.8%		
V_H7183.33.55							4	7.3%
V_H7183.35.57	1	1.8%						
V_H7183.37.59					1	1.8%	1	1.8%
V_H7183.46.75					2	3.6%	2	3.6%
V_H7183.47.76					5	8.9%	7	12.7%
Total	55	100%	56	100%	56	100%	55	100%

Table S3. Primer list, related to Figures 1-6, S1-10.

3C		
Name	Sequence (5'-3')	Reference
7183.4.6	ATTGCACTGAATGTGTAGATTG	
V_H81X	CTGGCTACTGCTTTTGATTTAA	
7183.1.1	GATGTACTTTTGCTAAGTCTGC	
IGCR1	GGATGTGAGTAGCTAGAGGATA	
Eμ	GGAACAATTCCACACAAAGACTC	(Guo et al., 2011a)
HS4	GTAGGAAGAGTCATTCTTGACC	
Eμ (+20)	ATACATGAACACCTCTCTCTCT	
HS4 (-21)	TCTAAACTCTCAACCCAGAGTA	
HS4 (+19)	CCAAAATTCTCAACCAGGAAAC	
α-amylase-F	GCTTCCATGATACTCTATGTTCTTCCT	(Guo et al., 2011a)
α-amylase-R	GAGATCTTACGTAGGCACTTAGTGGTATAA	(Guo et al., 2011a)
Eμ probe	AGCTTTAAGAGCAGCAGCCACAGCT	(Guo et al., 2011a)
V_H81X probe	TCAGAAGTAAAGCCAAGAGCTTACATC	
α-amylase probe	TTGAATATGTACCGAGTACACATGGATGGTGCAT	(Guo et al., 2011a)
FISH		
V_H81X-F	GTCTCTGTGTTGTTCTATGTCT	
V_H81X-R	TAGTAGATGAAACTACCATCAG	
IGCR1-F	CATCAGAAACAACAGCATCTCC	
IGCR1-R	GGAACATCGTGTCTGTGTTTGT	
5'7183-F	TTGGCTCACTCTGAGTTGGGATTCCTC	(Guo et al., 2011a)
5'7183-R	TAAAGCTGAACAAGGACCACAAGACGA	(Guo et al., 2011a)
3'558-F	AAGTCCCTGGGAGCTCTGGGGCAGTCA	(Guo et al., 2011a)
3'558-R	TTGTTTCTAGGAAAAGATAGGCACACAGAT	(Guo et al., 2011a)
V10-3-F	GCACATCTTCATTGTTCTTCTGAAATC	(Guo et al., 2011a)
V10-3-R	CTGACCCAGCCTACTGAAGA GTCAAAC	(Guo et al., 2011a)
V10-F	CACCTCCAATAGCACTCACAGGTTGGC	(Guo et al., 2011a)
V10-R	CAAAGGCTGCCTGCACTAAGACTGGTG	(Guo et al., 2011a)
Eμ-F	AGCTCATGGTACTTTGAGGAAATC	
Eμ-R	TTGTAGGAGGACTTCCCTAATCTG	
ChIP/RNA/real-time PCR		
YY1-F	AAGATATTGACCATGAAACA	
YY1-R	CATGAGGGCAAGCTATTGTTC	
CTCF-F	GCGCCCGTTCCAGTGCAGTTTGTG	(Verma-Gaur et al., 2012)
CTCF-R	GCATAAGGCTTCTCCCCCGTGTGA	(Verma-Gaur et al., 2012)
V_H81X-F	ATTAATGGCTGCGACCAACT	(Guo et al., 2011b)
V_H81X-R	GCTTAGTGCAGCCTGGAGAG	(Guo et al., 2011b)
γ-actin-F (Figure 2)	GGTGTCCGGAGGCACTCTT	(Chakraborty et al., 2007)
γ-actin-R (Figure 2)	TGAAAGTGGTCTCATGGATACCA	(Chakraborty et al., 2007)
DQ52-F (Figure 2)	TGGTGCAAGGTTTTGACTAAGC	(Chakraborty et al., 2007)
DQ52-R (Figure 2)	CCAAACAGAGGGTTTTTGTTGAG	(Chakraborty et al., 2007)
5'Eμ-F	TTAACCGAGGAATGGGAGTG	(Degner et al., 2011)
5'Eμ-R	GGTGGGGCTGGACAGAGTGT	
3'Eμ-F	AATACCCGAAGCATTTACAGTGACT	

3’Eμ-R	AAGATTTGTGAAGCCGTTTTGACCA	
3’J558-F	GCCAGGCTTTCTACACCTTTTCC	(Guo et al., 2011a)
3’J558-R	CCTTGCCCTTGAACTTCTGATTG	(Guo et al., 2011a)
Q52.3.8-F	GTCTCAGGGTTCTCATTAACCAG	
Q52.3.8-R	GCTGAATGATAATTTGTGCTCCC	
7183.5.7-F	TAGTGACAGTGTCTGACTCAGG	
7183.5.7-R	GAGAGTATCACGGACCTTTCAG	
7183.4.6-F	AGGCCGGTCCTGGATTCGAGTT	
7183.4.6-R	TCACTAACAAAACAAACAACAA	
7183.3.5-F	GGCCTGACTGTGCAGGTAGTCAC	
7183.3.5-R	GAAGGATCTCATGTCTATGAATT	
V_H81X(2)-F	TCCAGAGACAATACCAAGAAG	
V_H81X(2)-R	TTGAGCTCACAGTAACTTTTG	
V_H81X(1)-F	ATTAATGGCTGCGACCAACT	(Guo et al., 2011b)
V_H81X(1)-R	GCTTAGTGCAGCCTGGAGAG	(Guo et al., 2011b)
Q52.1.2-F	CAGAGCATGACTGTGCTAGAG	
Q52.1.2-R	GACGTGTCTTAGTCCCTCTACT	
71823.1.1-F	TGCCCAAGTCTAACTCCAAAG	
71823.1.1-R	GGGCTCCTTTGTCACAACT	
IG1-F	ATCTTGTGAAAATGGATCAGCC	
IG1-R	ACAAACTTTCATCTACTGTTGA	
IG2-F	GCGAAGTAGCATGGTCTTAGTT	
IG2-R	TGCTCAGTCAACAGCCATCAG	
DFL16.1-F (Figure 5)	ACACCTGCAAAACCAGAGACCATA	(Subrahmanyam et al., 2012)
DFL16.1-R (Figure 5)	GATCTGACTTTAGGGTGGTTGGA	(Subrahmanyam et al., 2012)
DSP2-F (Figure 5)	TGTTACCTTACTTGGCAGGGATTT	(Subrahmanyam et al., 2012)
DSP2-R (Figure 5)	TGGGTTTTTGTTGCTGGATATATC	(Subrahmanyam et al., 2012)
J_H2-F	TACTTTGACTACTGGGGC	(Chakraborty et al., 2009)
J_H2-R	CCCTAGTCCTTCATGACC	(Chakraborty et al., 2009)
V_H81X(-4)-F	GGAACGAGAACAGAAACCCTAA	
V_H81X(-4)-R	CTTTCTTCTCCTGCCCTTACTC	
V_H81X(+4)-F	GTCCTCCATTTCTCTCAGTGTG	
V_H81X(+4)-R	GAATAGTTGCAAGTGGGCTTTG	
DFL16.1(-4)-F	CCTCCTTGACAGCCTTGGGG	
DFL16.1(-4)-R	GTCACTCCCTCCTCCCTGTTG	
DFL16.1(-1.7)-F	GGCGAAGAAGCTTGTATCACAT	(Chakraborty et al., 2007)
DFL16.1(-1.7)-F	GTGGGTGGGATCAGTGCCCATCTTA	(Chakraborty et al., 2007)
DFL16.1-F (Figure S1D)	CAAAGCAGCCACCATCCAG	(Chakraborty et al., 2007)
DFL16.1-R (Figure S1D)	GCAGCACGGTTGAGTTTCAG	(Chakraborty et al., 2007)
DSP2-F (Figure S1D)	CAACAAAAACCCAGTATGCCCAG	(Chakraborty et al., 2007)
DSP2-R (Figures 5, S1D)	GTGCTTTCACCTGT TGTGGG	(Chakraborty et al., 2007)
DQ52-F (Figures 5, S1D)	CCCTGTGGTCTCTGACTGGTG	(Chakraborty et al., 2007)
DQ52-R (Figure S1D)	GATTTCTCAAGCCTCTCTACTTCCTC	(Chakraborty et al., 2007)
Eμ-F	GGAATGGGAGTGAGGCTCTCTC	(Chakraborty et al., 2007)
Eμ-R	CTGCAGGTGTTCTGGTTCTGATCGG	(Chakraborty et al., 2007)
Cγ3-F	TGGACAAACAGAAGTAGACATGGGTC	(Subrahmanyam et al., 2012)

Cγ3-R	GGGGTTTAGAGGAGAGAAGGCAC	(Subrahmanyam et al., 2012)
HS6-F	CCGCCCTTCACACCCTGACAAAC	(Subrahmanyam et al., 2012)
HS6-R	CTGGCACTGAGCAAGCAAACTCT	(Subrahmanyam et al., 2012)
γ-actin-F (Figures 5, S1D)	GACACCCAACCCCGTGACG	(Guo et al., 2011a)
γ-actin-R (Figures 5, S1D)	GCGGCCATCACATCCCAG	(Guo et al., 2011a)
DFL16.1(-4.5)-F	AGGCATCTCATCTCACTCTAAGC	(Subrahmanyam et al., 2012)
DFL16.1(-4.5)-R	TGTGTCCCTCTAAGACGAGTGAAT	(Subrahmanyam et al., 2012)
DFL16.1-F (Figure S1E)	AACTCAACCGTGCTGCCTG	(Chakraborty et al., 2007)
DFL16.1-R (Figure S1E)	CAATGGGTTTTTGCTGATGG	(Chakraborty et al., 2007)
Cμ-F	AGAGATCTGCATGTGCCCATT	(Bolland et al., 2007)
Cμ-R	TGGTGGGACGAACACATTTACA	(Bolland et al., 2007)
RAG2-F	TGTGCTACATCATATATTCTCC	
RAG2-R	TACTGGCAAGTGAGTGTCCTCC	
PAIR-F	GAGCTCTCCTTCAGTTCTTGAAT	(Ebert et al., 2011)
PAIR-R	TCTGCACTGTGTGACAATGG	(Ebert et al., 2011)
DJ/VDJ recombination assay		
DFL16.1-F	ACA CCT GCA AAA CCA GAG ACC ATA	
DSP-F	ATG GCC CCT GAC ACT CTG CAC TGC TA	
DQ52-F	GCGACTGTTTTGAGAGAAATCATTGG	(Subrahmanyam et al., 2012)
J_H4-R	GGGTCTAGACTCTCAGCCGGCTCCCTCAGGG	(Subrahmanyam et al., 2012)
ROSA26-F	AAAGTCGCTCTGAGTTGTTAT	
ROSA26-R	GGAGCGGGAGAAATGGATATG	
V_H7183	GTGGAGTCTGGGGGAGGCTTA	(Guo et al., 2011b)
V_HQ52	CTCACAGAGCCTGTCCATCAC	(Guo et al., 2011b)
V_HJ558	ARGCCTGGGRCTTCAGTGAAG	(Guo et al., 2011b)
J_H1-R	TGAGGAGACGGTGACCGTGGTCCC	
V_H81X	GGAGTTGGTCGCAGCCATTAATAGT	(Guo et al., 2011b)
DQ52-R	CATCCACCCTTCTGATGCTTGCATT	(Guo et al., 2011b)
PCR		
Eμ-F (Figure S2C)	GGACCACCTCTGTGACAGCATT	
Eμ-R (Figure S2C)	AGAGGGAGTTCACACAGAGCAT	
IGCR-F (Figure S5B)	CTATCTGGGTACCTGTGAACTCT	
IGCR-F (Figure S5B)	CGTATGAGCCATCTCAGCTCAG	
C1-F (Figure S6E)	CTGAAACTCTCCTGTGAATCCAA	
C1-F (Figure S6E)	CTGGTGCTCAAGCAGATTCA	
C2-F (Figure S6E)	CACTATCTACAGAGATGATGCC	
C2-R (Figure S6E)	ATTCTGAGCTGCCTTTTCTGAA	
gRNA target sequence		
Eμ-1	TTACTCTTAAGTTGGTTCCT	
Eμ-2	ATACCCGAAGCATTTACAGT	
IGCR1-1	GGAAAACTCTGTAGGACTAC	(Hu et al., 2015)
IGCR1-2	TGGGACATGTAAACTGTAAC	(Hu et al., 2015)
C1-1	TGGAGAGACGATTCATCATC	
C1-2	TGATGATTGACTACCAAACC	
C2-1	GAGCTGGGCTTCCTTGCAAT	
C2-2	CGTTTACCTTACAAAAACCC	

Table S4. Barcode sequence for different cell lines, related to Figure 6.

CBE$^{-/-}$(1)	CGAACTGT
	CTCTGTCT
	GATGGAAT
CBE$^{-/-}$(2)	ATATAGGA
	CACGTGTT
CBE$^{-/-}$(1)/C1$^{-/-}$	ATCGCCAG
	CATTCCAA
CBE$^{-/-}$(1)/C2$^{-/-}$	CAGGAGGC
	CGACTGGG
CBE$^{-/-}$(1)/C1$^{-/-}$C2$^{-/-}$	GGCAGACG
	CACAGTTG

Table S5. V_H utilization in different cell lines, related to Figure 6.

V_Hs	CBE$^{-/-}$(1)			CBE$^{-/-}$(2)		CBE$^{-/-}$(1)/C1$^{-/-}$		CBE$^{-/-}$(1)/C2$^{-/-}$		CBE$^{-/-}$(1)/C1$^{-/-}$C2$^{-/-}$	
V_H7183.a1psi.1	742	883	887	2059	1506	282	390	789	5869	1066	3221
V_HQ52.a1psi.2	0	0	0	0	0	0	0	1	0	0	0
V_H7183.a2.3	10999	9886	16829	80949	69137	10	12	29255	188408	12	19
V_HQ52.a2.4	262	296	316	1951	1228	1872	3178	0	0	0	0
V_H7183.a3psi.5	0	0	0	0	0	0	0	0	0	0	0
V_H7183.a4.6	54	78	76	440	243	248	358	758	5681	18583	48752
V_H7183.a5psi.7	0	0	0	0	0	0	0	0	0	0	0
V_HQ52.a3.8	20	9	35	134	82	55	61	79	685	1748	4632
V_H7183.a6psi.9	0	0	0	0	0	0	0	0	0	0	0
V_H7183.a7.10	2	5	5	60	35	1	12	9	125	181	592
V_H7183.a8psi.11	0	0	0	0	0	0	0	0	0	0	0
V_HQ52.a4psi.12	0	0	0	0	0	0	0	0	0	0	0
V_HQ52.a5.13	0	0	0	3	3	0	1	1	9	8	27
V_H7183.a9psi.14	0	0	0	0	0	0	0	0	0	0	0
V_H7183.a10.15	0	0	0	7	4	0	0	1	11	15	65
V_H7183.a11psi.16	0	0	0	0	0	0	0	0	0	0	0
V_HQ52.a6psi.17	0	0	0	0	0	0	0	0	0	0	0
V_HQ52.a7.18	0	0	0	0	0	0	0	0	0	0	0
V_H7183.a12psi.19	0	0	0	0	0	0	0	0	0	0	0
V_H7183.a13.20	0	2	1	21	9	1	1	1	19	26	11
$V_H$relic.a1psi.21	0	0	0	0	0	0	0	0	0	0	0
V_HQ52.a8.22	0	0	0	0	0	0	0	0	0	0	0
V_H7183.a14psi.23	0	0	0	0	0	0	0	0	0	0	0
V_H7183.a15.24	0	0	0	0	0	0	0	0	0	0	0
$V_H$relic.a2psi.25	0	0	0	0	0	0	0	0	0	0	0
V_HQ52.a9.26	0	0	0	0	0	0	0	0	0	0	0
V_H7183.a16.27	0	0	0	6	0	0	0	0	2	0	0
V_H7183.a17psi.28	0	0	0	0	0	0	0	0	0	0	0
V_HQ52.a10psi.29	0	0	0	0	5	0	0	0	0	1	4
V_H7183.a18psi.30	0	0	0	0	0	0	0	0	0	0	0
V_H7183.a19.31	0	0	0	0	0	0	0	0	0	0	1
V_HQ52.a11psi.32	0	0	0	0	0	0	0	0	0	0	0
V_HQ52.a12.33	0	0	0	0	0	0	0	0	0	0	0
V_H7183.a20psi.34	0	0	0	0	0	0	0	0	0	0	0
V_H7183.a21.35	0	0	2	1	3	0	0	0	4	0	0
V_H7183.a22psi.36	0	0	0	0	0	0	0	0	0	0	0
V_HQ52.a13.37	0	0	0	3	0	0	0	0	0	0	0
V_HQ52.a14psi.38	0	0	0	0	0	0	0	0	0	0	0
V_H7183.a23psi.39	0	0	0	0	0	0	0	0	0	0	0
V_H7183.a24.40	2	0	0	1	3	0	0	1	1	2	0
$V_H$relic.a3psi.41	0	0	0	0	0	0	0	0	0	0	0

V_Hs	CBE$^{-/-}$(1)			CBE$^{-/-}$(2)		CBE$^{-/-}$(1)/C1$^{-/-}$		CBE$^{-/-}$(1)/C2$^{-/-}$		CBE$^{-/-}$(1)/C1$^{-/-}$C2$^{-/-}$	
V_HQ52.a15.42	0	0	0	0	0	0	0	0	0	0	0
V_H7183.a25.43	0	0	0	0	0	0	0	0	2	0	9
V_H7183.a26psi.44	0	0	0	0	0	0	0	0	0	0	0
V_HQ52.a16psi.45	0	0	0	0	0	0	0	0	0	0	0
V_HQ52.a17.46	0	0	0	0	0	0	0	0	0	0	0
V_H7183.a27psi.47	0	0	0	0	0	0	0	0	0	0	0
V_H7183.a28.48	0	0	0	0	0	0	0	0	0	1	0
V_H7183.a29psi.49	0	0	0	0	0	0	0	0	0	0	0
V_H7183.a30.50	0	0	0	0	2	0	0	0	0	0	0
$V_H$relic.a4psi.51	0	0	0	0	0	0	0	0	0	0	0
V_HQ52.a18.52	2	0	0	1	0	0	0	0	0	0	0
V_H7183.a31psi.53	0	0	0	0	0	0	0	0	0	0	0
V_H7183.a32psi.54	0	0	0	0	0	0	0	0	0	0	0
V_H7183.a33.55	0	0	0	0	0	0	0	0	0	0	0
V_H7183.a34psi.56	0	0	0	0	0	0	0	0	0	0	0
V_H7183.a35.57	0	0	0	0	0	0	0	0	0	0	0
V_H7183.a36psi.58	0	0	0	0	0	0	0	0	0	0	0
V_H7183.a37.59	0	0	0	4	5	0	0	0	0	0	3
V_H7183.a38psi.60	0	0	0	0	0	0	0	0	0	0	0
V_HQ52.a19.61	0	0	0	0	0	0	0	0	0	0	3
V_HQ52.a20psi.62	0	0	0	0	0	0	0	0	0	0	0
V_HQ52.a21.63	0	0	0	2	1	0	0	0	0	0	0
V_H7183.a39psi.64	0	0	0	0	0	0	0	0	0	0	0
V_H7183.a40psi.65	0	0	0	0	0	0	0	0	0	0	0
V_H7183.a41psi.66	0	0	0	0	0	0	0	0	0	0	0
V_HQ52.a22.67	0	0	0	0	0	0	0	0	0	0	0
V_HQ52.a23.68	0	0	0	0	0	0	0	0	0	0	0
V_H7183.a42psi.69	0	0	0	0	0	0	0	0	0	0	0
V_H7183.a43psi.70	0	0	2	0	1	0	0	0	0	0	0
V_H7183.a44psi.71	0	0	0	0	0	0	0	0	0	0	0
V_HQ52.a24.72	0	0	0	0	3	0	0	0	0	0	0
V_H7183.a45psi.73	0	0	0	0	0	0	0	0	0	0	0
V_HQ52.a25psi.74	0	0	0	0	0	0	0	0	0	0	0
V_H7183.a46.75	0	0	0	4	0	0	0	0	4	0	0
V_H7183.a47.76	0	0	0	7	1	0	0	2	7	1	1
V_H7183.a48psi.77	0	0	0	1	0	0	0	0	0	0	0
V_HQ52.a26psi.78	0	0	0	0	0	0	0	0	0	0	0
V_HQ52.a27.79	0	0	0	0	1	0	0	0	4	0	2
V_H7183.a49psi.80	0	0	0	0	0	0	0	0	0	0	0
V_HS107.a1.81	0	0	0	0	3	0	0	0	4	2	0
V_HS107.a2psi.82	0	0	0	0	0	0	0	0	0	0	0
V_HSM7.a1.83	0	0	0	0	0	0	0	0	0	0	0
V_HX24.a1.84	0	0	0	0	0	0	0	0	0	0	0

V_Hs	CBE$^{-/-}$(1)			CBE$^{-/-}$(2)		CBE$^{-/-}$(1)/C1$^{-/-}$		CBE$^{-/-}$(1)/C2$^{-/-}$		CBE$^{-/-}$(1)/C1$^{-/-}$C2$^{-/-}$	
V_H36-60.a1.85	0	0	0	0	0	0	0	0	0	0	0
$V_H$relic.a5psi.86	0	0	0	0	0	0	0	0	0	0	0
V_H11.a1.87	0	0	0	1	0	0	0	0	0	0	0
V_HSM7.a2psi.88	0	0	0	0	0	0	0	0	0	0	0
V_HX24.a2.89	0	0	0	0	0	0	0	0	5	0	0
V_H36-60.a2.90	1	2	0	0	0	0	0	0	0	3	1
$V_H$relic.a6psi.91	0	0	0	0	0	0	0	0	0	0	0
V_H11.a2.92	0	0	0	0	0	0	0	1	1	0	0
V_HSM7.a3.93	0	0	0	0	1	0	0	0	0	0	0
$V_H$relic.a7psi.94	0	0	0	0	0	0	0	0	0	0	0
V_H3609N.a1psi.95	0	0	0	0	0	0	0	0	0	0	0
V_HGAM3-8.a1.96	0	0	0	0	0	0	0	0	0	0	0
V_H12.a1psi.97	0	0	0	0	0	0	0	0	0	0	0
V_HGAM3-8.a2.98	0	0	0	0	0	0	0	0	0	0	0
V_H12.a2psi.99	0	0	0	0	0	0	0	0	0	0	0
V_HGAM3-8.a3.100	0	0	0	0	0	0	0	0	0	0	0
V_H12.a3.101	0	0	0	0	0	0	0	0	9	0	0
V_HGAM3-8.a4.102	0	0	0	0	0	0	0	0	0	0	0
V_H12.a4psi.103	0	0	0	0	0	0	0	0	0	0	0
V_H12.a5psi.104	0	0	0	0	0	0	0	0	0	0	0
V_HGAM3-8.a5.105	0	0	0	3	0	0	0	0	1	0	0
V_HS107.a3.106	0	0	0	14	11	0	0	0	0	2	0
V_H15.a1psi.107	0	0	0	0	0	0	0	0	0	0	0
V_HSM7.a4.108	0	0	0	1	1	0	0	0	1	0	0
V_H36-60.a3psi.109	0	1	0	0	0	0	0	0	0	0	0
V_HS107.a4.110	0	0	0	0	0	0	0	0	0	0	0
V_H36-60.a4.111	0	0	0	0	0	0	0	1	0	0	0
V_H36-60.a5.112	0	0	0	0	0	0	0	0	0	0	0
V_H3609N.a2psi.113	0	0	0	0	0	0	0	0	0	0	0
V_H36-60.a6.114	0	0	0	0	0	1	0	0	0	6	0
V_HGAM3-8.a6.115	0	1	0	0	0	0	0	0	0	0	3
V_H36-60.a7psi.116	0	0	0	0	0	0	0	0	0	0	0
V_H36-60.a8.117	0	0	0	0	0	0	0	0	0	0	0
V_HJ606.a1psi.118	0	0	0	0	0	0	0	0	0	0	0
V_HJ558.a1psi.119	0	0	0	0	0	0	0	0	0	0	0
V_H3609N.a3.120#	0	0	0	3	10	0	0	0	1	0	0
V_H36-60.a9.121#	0	0	0	0	0	0	0	0	0	0	0
V_HJ606.a2psi.122#	0	0	0	0	0	0	0	0	0	0	0
V_H36-60.a10.123#	0	0	0	0	0	0	0	0	1	0	0
V_HJ606.a3.124#	0	0	0	0	0	0	0	0	0	0	0
V_HJ606.a4.125#	0	0	0	0	0	0	0	0	0	0	0
V_HJ606.a5psi.126#	0	0	0	0	0	0	0	0	0	0	0
V_HJ606.a6.127#	0	0	0	0	0	0	0	0	0	0	0
V_HJ606.a7.128#	0	0	0	1	0	0	0	0	0	1	0